Elastic α-^{12}C scattering at low energies in effective field theory

Shung-Ichi Ando

Sunmoon University, Asan, Republic of Korea

Outline

- Introduction: ^{12}C$(\alpha, \gamma)^{16}$O process in the stars
- EFT for the radiative capture and elastic scattering of the α-^{12}C system at low energies
- A new renormalization method
- Numerical results
- Summary

1. Introduction

- 90% of human body consists of ^{12}C and ^{16}O.
- ^{12}C and ^{16}O are synthesized during helium burning process in the stars.
- ^{12}C/^{16}O ratio in the universe is mostly determined by the ^{12}C$(\alpha,\gamma)^{16}$O process.
- Meanwhile about 20% uncertainty of S-factors of the ^{12}C$(\alpha,\gamma)^{16}$O process (NACRE-II) exists after more than a half century long intensive studies for the process.

The main goal is to determine S_{E1}-factor for the process with 5-10% theoretical uncertainty in the future studies.

^{12}C(α, γ)^{16}O process

- Level diagram of ^{16}O

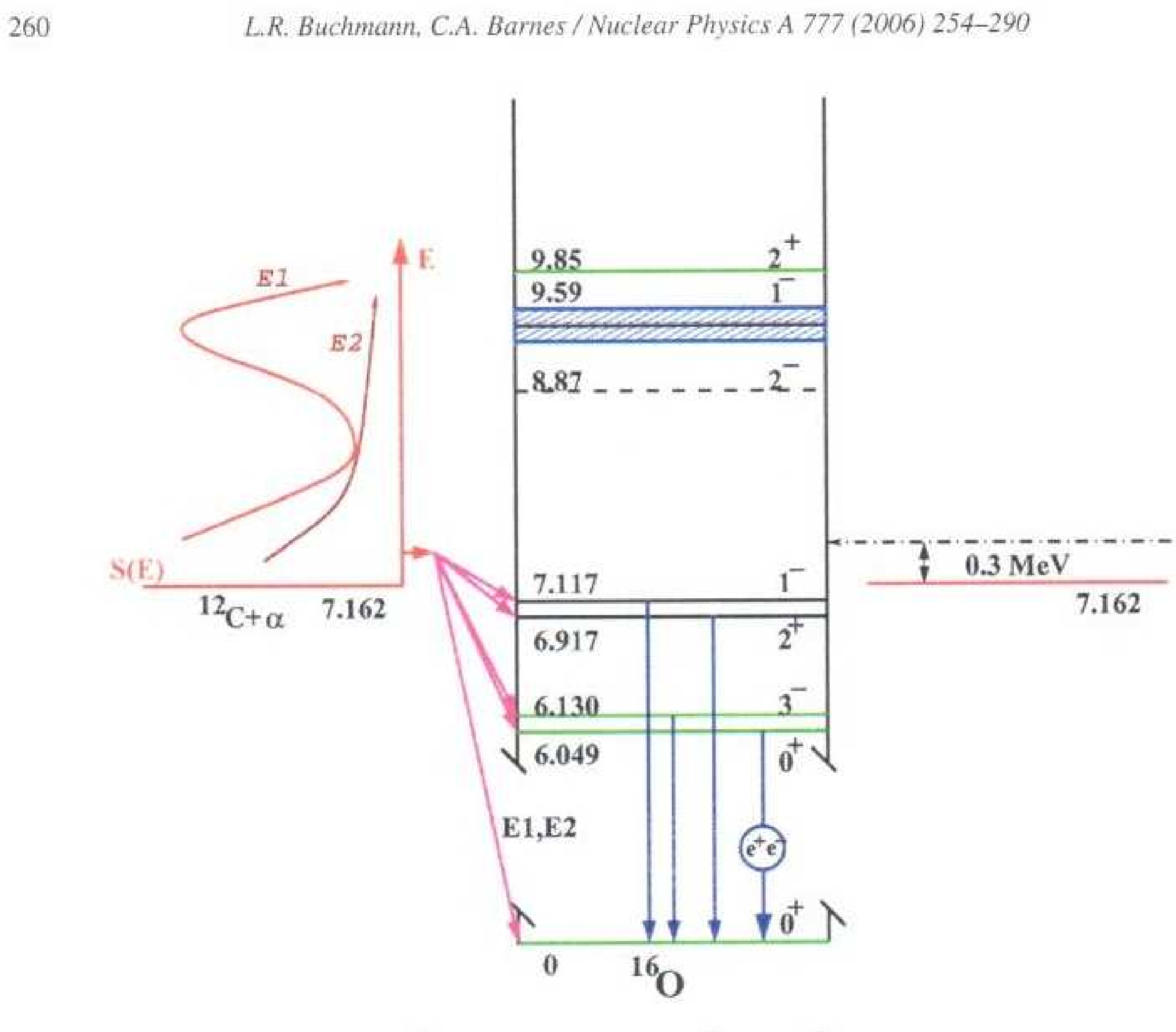

Fig. 1. ^{16}O states relevant to the ^{12}C(α, γ)^{16}O reaction.

- Effective Field Theories (EFTs)
  - Model independent approach
  - Separation scale
  - Counting rules
  - Parameters should be fixed by experiments

2. ^{12}C(α,γ)^{16}O in EFT

- Typical momentum of the process
  at $T_G \simeq 0.3$ MeV; $Q \sim \sqrt{2\mu T_G} \sim 40$ MeV
  The α and ^{12}C states; elementary-like states
- Separation (large) scale
  Excited energies of α and ^{12}C; large scale
  The large momentum scale, $\Lambda_H \sim 150$ MeV
- Expansion parameter, $Q/\Lambda_H \sim 1/3$
  Thus, 5% uncertainty can be achieved up to N^{3}LO

- Diagrams for ^{12}C$(\alpha,\gamma)^{16}$O process

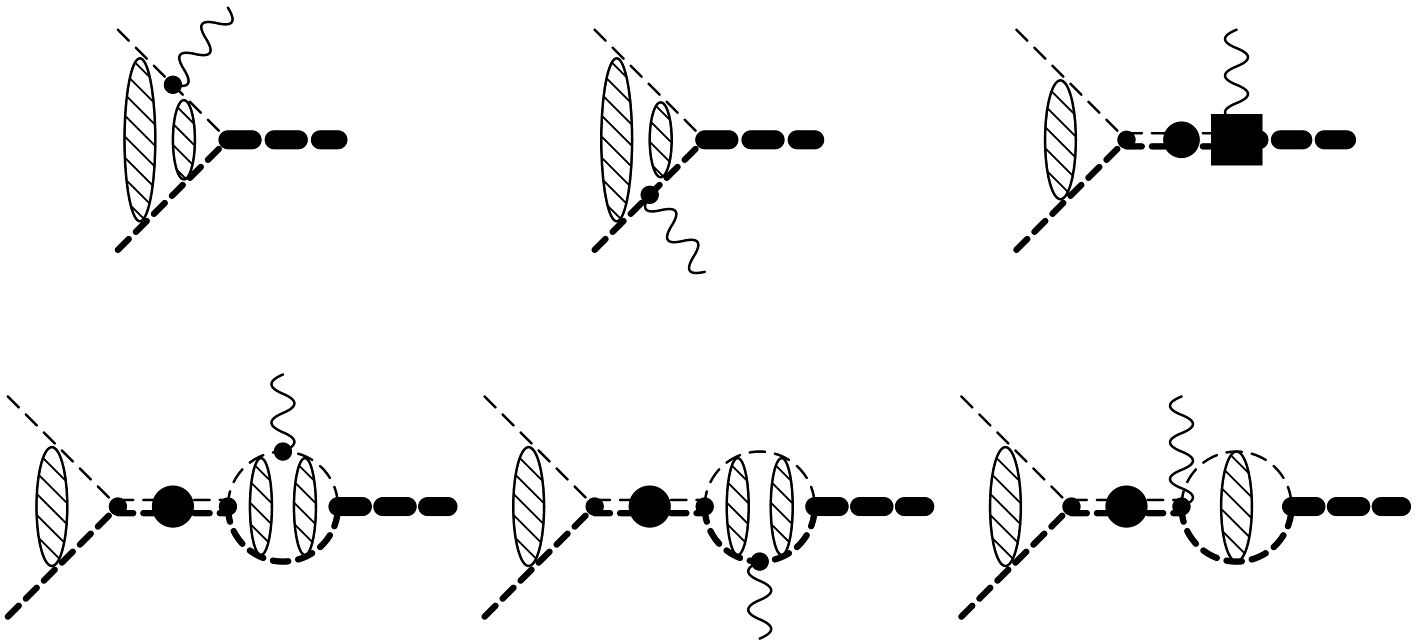

3. Elastic α-^{12}C scattering in EFT

- Typical scales:
  T_α, α energies of the exp. data (in Lab. frame) c.f., $T \simeq 4/3\,T_\alpha$
  $T_\alpha = 2.6 - 6.6$ MeV; $k = 105 - 170$ MeV
- Large scales:
  The resonance energies, T (in CM frame)
  $T = 4.89, 2.42, 2.68, 4.44$ MeV for $l^\pi_{i-th} = 0^+_3$, 1^-_2, 2^+_2, 3^-_2
  $k = 166, 117, 123, 136$ MeV
- Binding energies of ^{16}O:
  $B = 1.11, 0.045, 0.24, 1.03$ MeV for $l^\pi_{i-th} = 0^+_2, 1^-_1, 2^+_1, 3^-_1$
  are included.

Scattering amplitudes from EFT

- Diagrams for dressed composite ^{16}O propagator

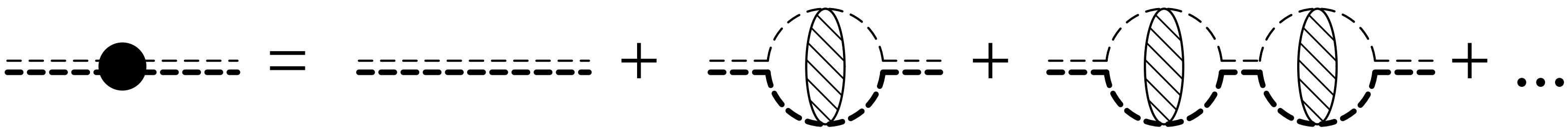

- Diagrams for elastic α-^{12}C scattering

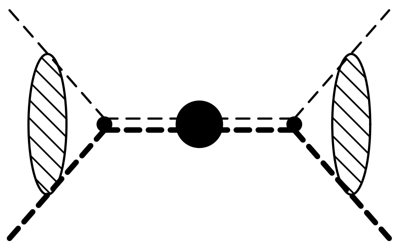

- Scattering amplitudes for l-th partial waves

$$A_l = \frac{2\pi}{\mu}\frac{(2l+1)P_l(\cos\theta)e^{2i\sigma_l}W_l(\eta)C_\eta^2}{K_l(k)-2\kappa H_l(k)} ,$$

where η is the Sommerfeld parameter, $\eta = \kappa/k$ where κ is the inverse of the Bohr radius, $\kappa = Z_2 Z_6 \mu\alpha = 245$ MeV, and

$$C_\eta^2 = \frac{2\pi\eta}{e^{2\pi\eta}-1} , \quad W_l(\eta) = \frac{\kappa^{2l}}{(l!)^2}\prod_{n=0}^{l}\left(1+\frac{n^2}{\eta^2}\right) , \quad H_l(k) = W_l(\eta)H(\eta) ,$$

with

$$H(\eta) = \psi(i\eta) + \frac{1}{2i\eta} - \ln(i\eta) .$$

$\psi(z)$ is the digamma function.

- The effective range parameters

$$K_l(k) = -\frac{1}{a_l} + \frac{1}{2} r_l k^2 - \frac{1}{4} P_l k^4 + Q_l k^6 - R_l k^8 + \cdots .$$

- The binding energies

The denominator of the scattering amplitude, $D_l(k)$, vanishes;

$$D_l(k_b) = K_l(k_b) - 2\kappa H_l(k_b) = 0 ,$$

at $k_b = i\gamma_l$ where γ_l is the binding momentum, $\gamma_l = \sqrt{2\mu B_l}$. Thus one has

$$-\frac{1}{a_l} = \frac{1}{2} r_l \gamma_l^2 + \frac{1}{4} P_l \gamma_l^4 + Q_l \gamma_l^6 + R_l \gamma_l^8 + \cdots + 2\kappa H_l(k_b) ,$$

and

$$D_l(k) = \frac{1}{2} r_l \left(k^2 + \gamma_l^2\right) - \frac{1}{4} P_l \left(k^4 - \gamma_l^4\right) + Q_l \left(k^6 + \gamma_l^6\right) - R_l \left(k^8 - \gamma_l^8\right) + \cdots$$
$$-2\kappa \left[H_l(k) - H_l(k_b)\right] .$$

- Fitting effective range parameters to phase shift data

$$W_l(\eta)C_\eta^2 k\cot\delta_l = ReD_l(k)\,.$$

- ANCs for the subthreshold states

$$|C_b| \quad = \quad \gamma_l^l \frac{\Gamma(l+1+|\eta_b|)}{l!}\left(\left|-\frac{dD_l(k)}{dk^2}\right|_{k^2=-\gamma_l^2}\right)^{-\frac{1}{2}} \quad (\mathrm{fm}^{-1/2})\,,$$

where $\eta_b = \kappa/k_b$.

A new renormalization method

- A mismatch of the power series: In the case of s-wave, for example, the reported phase shift at the smallest energy, $T_\alpha = 2.6$ MeV, is $\delta_0 = -1.893°$;

$$C_\eta^2 k \cot \delta_0 = ReD_0(k) = K_0(k) - 2\kappa ReH_0(k), ,$$

where $K_0(k)$ and $2\kappa ReH_0(k)$ are expanded as

$$\begin{aligned}
K_0(k) &= -\frac{1}{a_0} + \frac{1}{2} r_0 k^2 - \frac{1}{4} P_0 k^4 + Q_0 k^6 - R_0 k^8 + \cdots \, , \\
2\kappa ReH_0(k) &= \frac{1}{6\kappa} k^2 + \frac{1}{60\kappa^3} k^4 + \frac{1}{126\kappa^5} k^6 + \frac{1}{120\kappa^7} k^8 + \cdots \\
&= \frac{1}{2} \tilde{r}_0 k^2 - \frac{1}{4} \tilde{P}_0 k^4 + \tilde{Q}_0 k^6 - \tilde{R}_0 k^8 + \cdots \\
&= 7.441 + 0.136 + 0.012 + 0.002 + \cdots \ \text{(MeV)} \, , \\
C_\eta^2 k \cot \delta_0 &= -0.019 \ \text{MeV} \, ,
\end{aligned}$$

at $k = 104$ MeV ($T_\alpha = 2.6$ MeV), $\kappa = 245$ MeV, and $C_\eta^2 = 6 \times 10^{-6}$.

- Three parameters, r_l, P_l, Q_l for $l = 0, 1, 2$,
- Four parameters, r_l, P_l, Q_l, R_l for $l = 3$ as the counter terms.

Numerical results: S-wave

- Input data sets $\{S0, S1, S2\}$, $T_\alpha = 2.6 - 3.6, 3.8, 4.0$ MeV for $l = 0$,

	a_0 (fm)	r_0 (fm)	P_0 (fm^3)	Q_0 (fm^5)	ReD_{0G} (MeV)
$S0$	6.2×10^4	0.268514(3)	$-0.0343(4)$	0.0019(2)	$4.2(7) \times 10^{-3}$
$S1$	6.6×10^4	0.268514(3)	$-0.0342(3)$	0.0020(3)	$4.0(5) \times 10^{-3}$
$S2$	5.8×10^4	0.268513(3)	$-0.0345(2)$	0.0018(1)	$4.4(4) \times 10^{-3}$
	—	$\tilde{r}_0$ (fm)	$\tilde{P}_0$ (fm^3)	$\tilde{Q}_0$ (fm^5)	—
	—	0.268735	-0.0349	0.0027	—

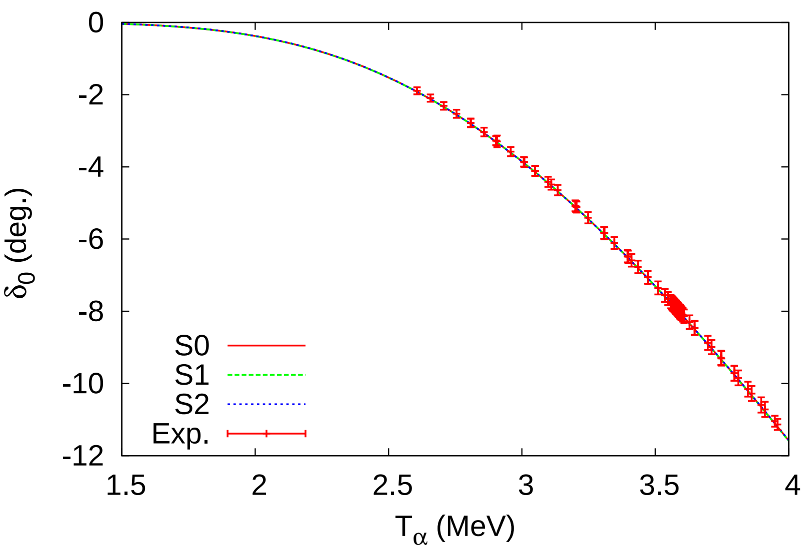

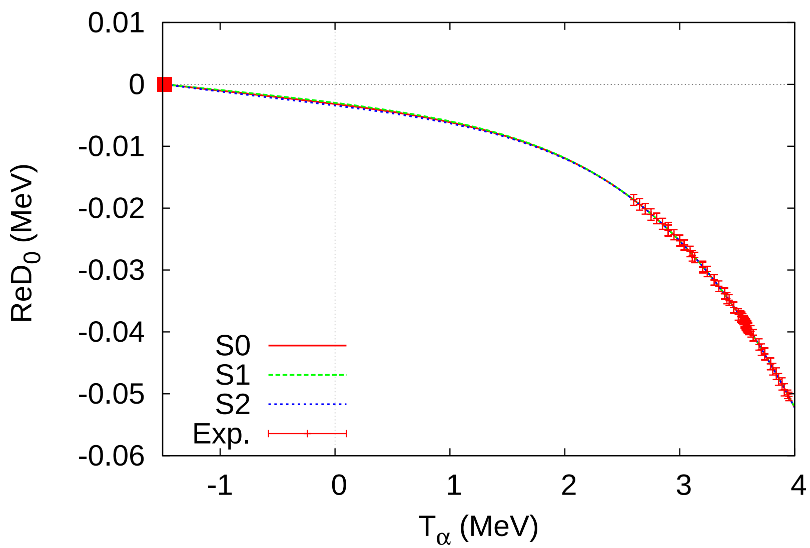

P-wave

- Input data sets $\{P0, P1, P2\}$, $T_\alpha = 2.6 - 3.0, 3.1, 3.2$ MeV for $l = 1$,

	a_1(fm^3)	r_1 (fm^{-1})	P_1 (fm)	Q_1 (fm^3)	ReD_{1G} (MeV^3)	$\|C_b\|$ (fm$^{-1/2}$)
$P0$	-1.8×10^5	0.4150(6)	$-0.577(8)$	0.019(3)	$2.7(8) \times 10^2$	$1.9(4) \times 10^{14}$
$P1$	-1.6×10^5	0.4153(2)	$-0.574(2)$	0.020(1)	$3.0(3) \times 10^2$	$1.8(1) \times 10^{14}$
$P2$	-1.3×10^5	0.4157(2)	$-0.569(2)$	0.023(1)	$3.5(3) \times 10^2$	$1.6(1) \times 10^{14}$
	—	$\tilde{r}_1$ (fm^{-1})	$\tilde{P}_1$ (fm)	$\tilde{Q}_1$ (fm^3)	—	—
	—	0.4135	-0.591	0.013	—	—

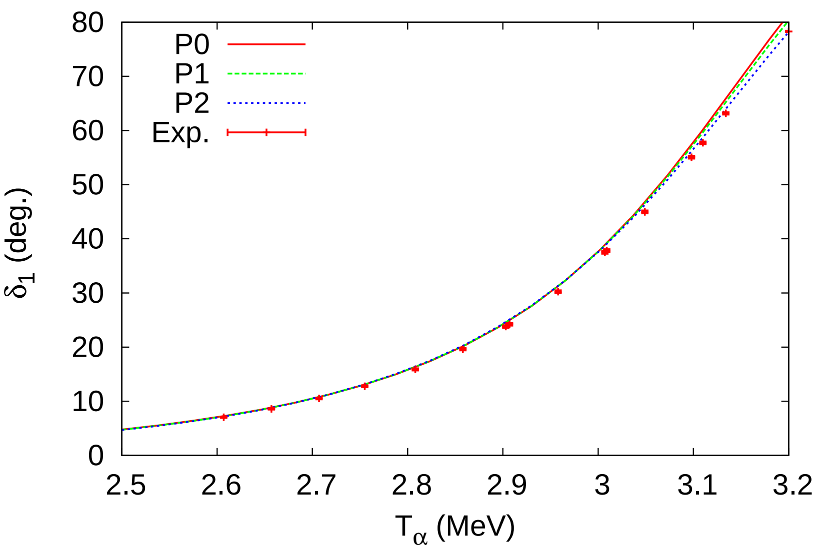

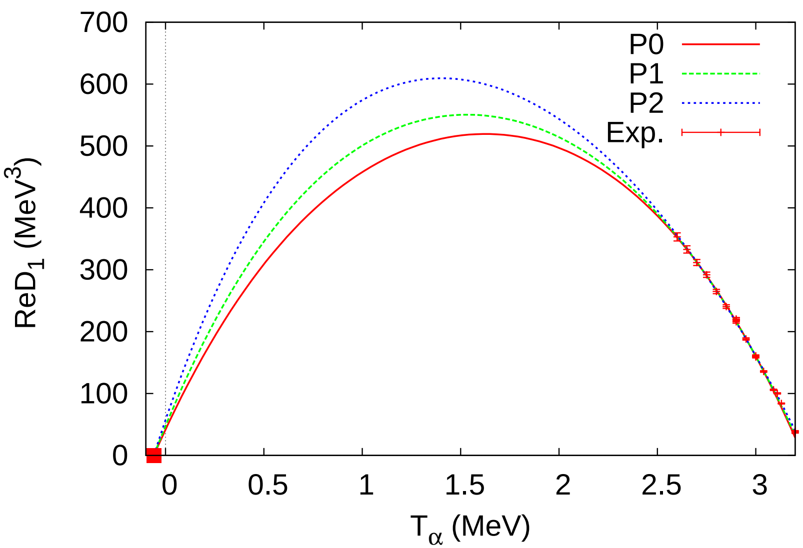

D-wave

- Input data sets $\{D0, D1, D2\}$, $T_\alpha = 2.6 - 3.0, 3.1, 3.2$ MeV for $l = 2$,

	a_2(fm^5)	r_2 (fm^{-3})	P_2 (fm^{-1})	Q_2 (fm)	ReD_{2G} (fm^{-5})	$\|C_b\|$ (fm$^{-1/2}$)
$D0$	10.3×10^3	0.155(4)	$-1.12(7)$	0.11(3)	$-1.66(156) \times 10^{-4}$	$2.4(3) \times 10^4$
$D1$	6.5×10^3	0.152(2)	$-1.16(4)$	0.08(2)	$-2.6(9) \times 10^{-4}$	$2.3(2) \times 10^4$
$D2$	4.3×10^3	0.149(2)	$-1.21(3)$	0.06(1)	$-3.8(6) \times 10^{-4}$	$2.1(1) \times 10^4$
	—	$\tilde{r}_2$ (fm^{-3})	$\tilde{P}_2$ (fm^{-1})	$\tilde{Q}_2$ (fm)	—	—
	—	0.159	-1.05	0.15	—	—

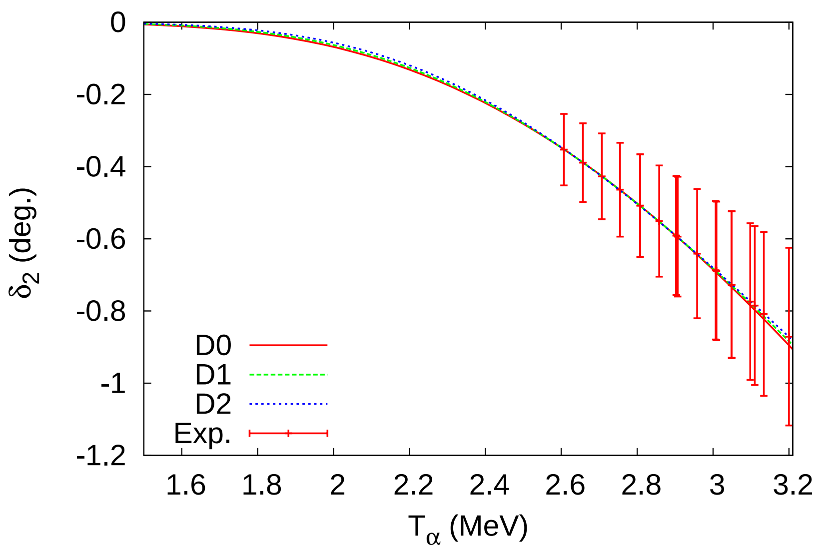

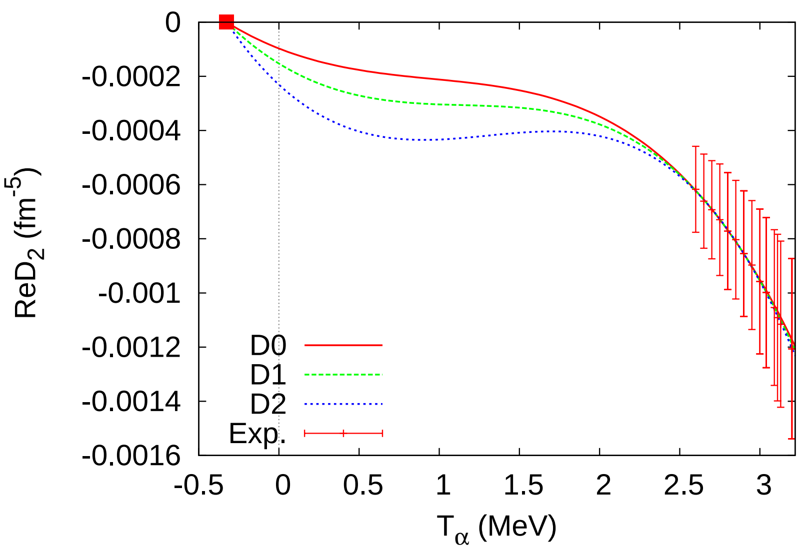

F-wave

- Input data sets $\{F0, F1, F2\}$, $T_\alpha = 2.6 - 4.6, 4.8, 5.0$ MeV for $l = 3$,

	a_3(fm^7)	r_3(fm^{-5})	P_3(fm^{-3})	Q_3(fm^{-1})	R_3(fm)	ReD_{3G} (fm^{-7})
$F0$	-1.4×10^3	0.0319(1)	$-0.453(11)$	0.317(9)	$-0.141(8)$	$7.8(8) \times 10^{-4}$
$F1$	-1.5×10^3	0.0320(1)	$-0.459(9)$	0.311(7)	$-0.146(6)$	$7.4(7) \times 10^{-4}$
$F2$	-1.8×10^3	0.0322(1)	$-0.472(7)$	0.301(6)	$-0.156(5)$	$6.4(6) \times 10^{-4}$
	—	$\tilde{r}_3$ (fm^{-5})	$\tilde{P}_3$ (fm^{-3})	$\tilde{Q}_3$ (fm^{-1})	$\tilde{R}_3$ (fm)	—
	—	0.0272	-0.498	0.290	-0.152	—

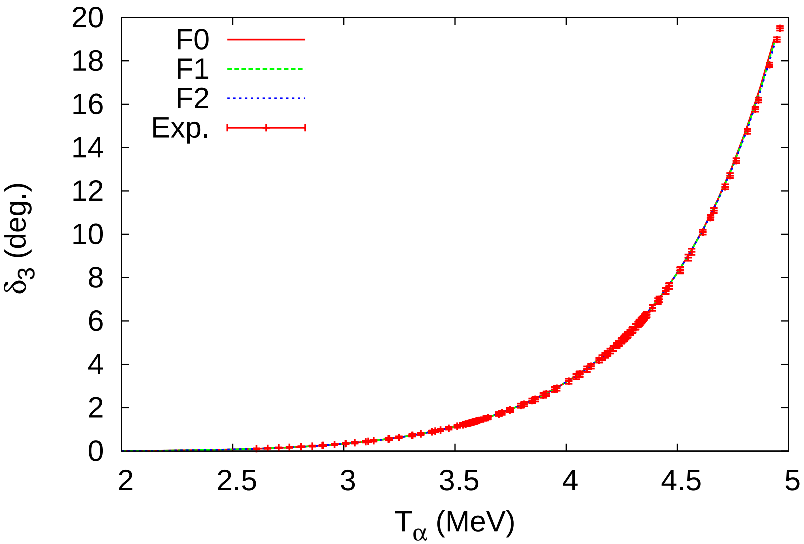

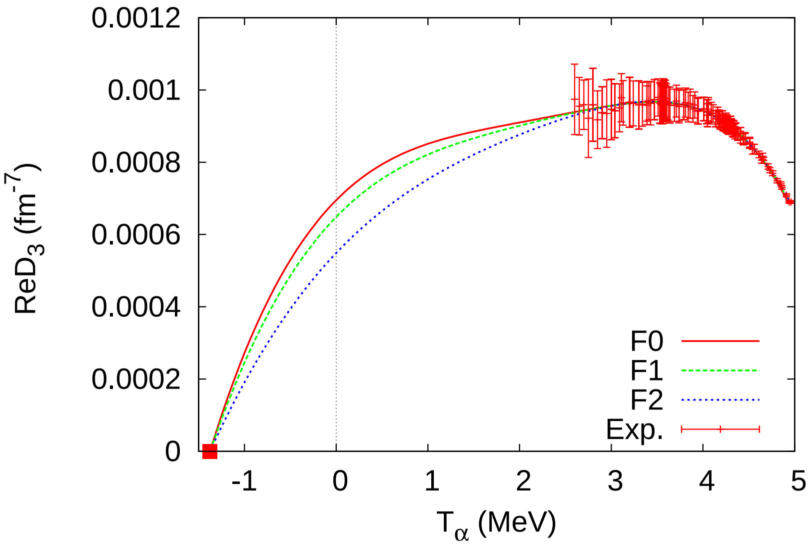

Convergence of the power series

- Expansion parameter $Q/\Lambda_H \sim 1/3$ at $Q \sim k_G = \sqrt{2\mu T_G}$,

$$\left(\frac{Q}{\Lambda_H}\right)^2 \sim 0.1\,, \quad \left(\frac{Q}{\Lambda_H}\right)^4 \sim 0.01\,, \quad \left(\frac{Q}{\Lambda_H}\right)^6 \sim 0.001\,.$$

- Ratios of the power series at T_G

l	$\lvert -\frac{1}{a_l}\rvert$	$\lvert\frac{1}{2}(r_l - \tilde{r}_l)k_G^2\rvert$	$\lvert -\frac{1}{4}(P_l - \tilde{P}_l)k_G^4\rvert$	$\lvert(Q_l - \tilde{Q}_l)k_G^6\rvert$
0	1	0.276	0.012	0.004
1	0.154	1	0.215	0.016
2	1	0.946	0.316	0.031
3	1	0.195	0.023	0.002

Results for ANCs

- ANC for the 1_1^- state
  - Our result:
    $(1.6 - 1.9) \times 10^{14}$ (fm$^{-1/2}$).
  - Exp. results: $(2.08 \pm 0.20) \times 10^{14}$ (Brune et al.),
    $(5.1 \pm 0.6) \times 10^{14}$ (Belhout et al.),
    $(17.4 - 26.4) \times 10^{14}$ (Adhikari and Basu).
  - Theor. results:
    $(2.22 - 2.24) \times 10^{14}$ (Katsuma),
    $2.14(6) \times 10^{14}$ (Ramirez Suarez and Sparenberg),
    2.073×10^{14} (Orlov et al.)

Results for ANCs

- ANC for the 2_1^+ state
  - Our result:
    $(2.1 - 2.4) \times 10^4$ (fm$^{-1/2}$)
  - Exp. results:
    $(11 \pm 1) \times 10^4$ (Brune et al.),
    $(34.5 \pm 0.5) \times 10^4$ (Belhout et al.),
    $(12.2 - 18.2) \times 10^4$ (Adhikari and Basu).
  - Theor. results:
    $(2.41 \pm 0.38) \times 10^4$ (Konig et al.),
    2.106×10^4 (Orlov et al,),
    $(14.45 \pm 0.85) \times 10^4$ (Sparenberg),
    $(12.6 \pm 0.5) \times 10^4$ (Dufour and Descouvemont),
    5.05×10^4 (Orlov et al.)

Summary

- EFT for the radiative capture and elastic scattering of α-^{12}C system at low energies is derived.
- The EFT is applied to the elastic α-^{12}C scattering at low energies introducing a new renormalization method.
- Experimental phase shifts below the resonance energies, including the 0_2^+, 1_1^-, 2_1^+, 3_1^- states, for $l = 0, 1, 2, 3$ are well reproduced by fitting three or four effective range parameters.
- Expansion series converge well, but significant uncertainties, about 10% for $l = 0, 3$, 30% for $l = 1$, 100% for $l = 2$, of the amplitudes interpolated to T_G remain.